CrossMark

ORIGINAL PAPER

Empirical equations for flood analysis in arid zones: the Ari-Zo model

Mohammad Albishi[1] · Jarbou Bahrawi[2] · Amro Elfeki[2]

Abstract Water resources all over the world are facing several problems such as scarcity, pollution, climate change, and global warming. Arid zones especially suffer from either severe drought or severe floods. Scientific analysis of flood events is difficult because of lacking flood measurement data and rainfall-runoff models that are suited for arid regions. Researchers in the field of hydrology are developing rainfall-runoff models for storm runoff predictions since 1932. However, it is noticeable that most research papers, books, and theses are considering studies in temperate regions, while arid zones are lacking such studies. The main objective of this paper is to derive a mathematical model called Ari-Zo, using regression analysis, to predict flood peaks, time to peak, and time of concentration from rainfall storms in arid zones. The data used in this study relied on storm measurements registered at Allith and Yiba basins and their subcatchments (eight subbasins) located in the southwestern part of Saudi Arabia. The stream flow data method has been used to derive the unit hydrograph in the Ari-Zo model from 36 storms. The study developed several mathematical relationships between the hydrological variables and the regional topography of the basins. The mathematical equations obtained from this study are the discharge peaking factor, time of concentration, and time to peak. The Ari-Zo model results are compared with the results of the National Resources Conservation Service (NRCS) method and showed substantial differences. The peaking factors of NRCS range between 0.0646 and 0.2582, while in Ari-Zo, it ranges between 0.0513 (low flood case) and 1.9465 (very extreme flood case). The ratio between the time to peak and the time of concentration in NRCS is equal to 0.667, while in Ari-Zo, it ranges between 0.05 and 0.5 and on average, it is 0.276. The parameters of time of concentration in Ari-Zo model are different from those of Kirpich equation. The study recommends using the Ari-Zo model for arid zone hydrological studies.

Keywords Arid zones · Empirical equations · Flood analysis · Hydrology · Unit hydrograph

✉ Mohammad Albishi
maalbeshi@kau.edu.sa

Jarbou Bahrawi
jbahrawi@kau.edu.sa

Amro Elfeki
aelfeki@kau.edu.sa

[1] Water Research Center, King Abdulaziz University, Jeddah, Saudi Arabia

[2] Department of Hydrology and Water Resource Management, Faculty of Meteorology, Environment, and Arid Land Agriculture, King Abdulaziz University, Jeddah, Saudi Arabia

Introduction

The study of the hydrological characteristics of the basins and developing of mathematical models for rainfall and runoff relationships that bind it with topographic characteristics are a very old subject. The first study of this topic was made by Sherman in 1932 (Sherman 1932 referenced by Viessman et al. 1977 and Viessman and Lewis 2002).

Since 1932, researchers are developing rainfall-runoff models for storm runoff predictions. However, it is noticeable that most researches, books, and theses are considering studies in temperate regions, while arid zones are lacking such studies.

Although the presence of severe storms in arid zones is rare, these storms happen a few times a year. The rare occurrence of the severe storms in arid zones and the lack of measurements of runoff render the study of the hydrological

Springer

characteristics in arid basins a difficult task. Recently in November 2009 (Al-watan online news 2010) and January 2011 (Alriyadh Newspaper 2011) in Jeddah city, there were extreme flood events that cause much damage in the city. Also, in May 2014 (Okaz Newspaper 2014) in Makkah Al-Mokarramah, severe flood events occurred.

Specialists and researchers in the field of water resources are developing methods and formulas to facilitate the process of calculating the relationship between rainfall and floods, so that they can predict future storms. Sherman (1932) was the first to develop method to study the concept of a unit hydrograph. Since then, many scientists, researchers, and some government institutions followed the same approach to find methods to estimate the flood hydrograph form a storm rainfall. There are four basic ways to drive the unit hydrograph, namely:

1. Derivation of unit hydrograph from stream flow data
2. Synthetic methods
3. Statistical distribution methods
4. Geomorphological instantaneous unit hydrograph.

In the stream flow data method, one must provide data on the rainfall strom and resulting flood hydrograh. Using this technique, the unit hydrograph from each flood can be derived. If there are sufficient records of rainfall events and corresponding floods, the results will be specific to that region.

Some of the synthetic methods are reviewed herein: Snydre's method (Snyder 1938 referenced by Viessman et al. 1977) has developed his own synthetic unit hydrograph in 1938 and has been used extensively by the US Corps of Engineers. In the Snyder method, two empirically defined terms, C_T and C_P, and the physiographic characteristics of the drainage basin are used to determine a D-hour unit hydrograph. A synthetic unit hydrograph that utilizes an instantaneous unit hydrograph (IUH) was developed in 1945 by Clark (Clark 1945 referenced by Viessman and Lewis 2002 and Raghunath 2006). A method of generating synthetic unit hydrograph for Midwestern watersheds has been developed by Gray in 1961 (Gray 1961 referenced by Viessman et al. 1977). National Resources Conservation Service (NRCS) in 1972 (Mockus 1957 and NRCS 1972 referenced by McCuen et al. 2002) presents a synthetic unit hydrograph procedure that has been widely used in flood control works.

In the statistical distribution methods, a two-parameter gamma distribution is used in the hydrologic applications. It has a long successful history that was started by Edson in 1951 (Edson 1951 referenced by Singh et al. 2011). It should be noted that the NRCS and Gray methods are dependent of their theory on the shape of the curve which resembles exactly the statistical distribution of the gamma distribution. This means that some of the synthetic methods are based on the shape of the statistical distributions. Bhunya et al. (2003) concluded that the two-parameter gamma distribution worked better in field data than the Gray, Snyder, and NRCS methods.

Since the aforementioned methods have been developed in temperate or humid regions, the current study is an attempt to derive equations for the arid region environment, specifically Saudi Arabia. Therefore, the main objective of this study is to derive a mathematical model called Ari-Zo (Albishi 2015) to predict flood hydrograph from rainfall storms in arid zones. The model is derived from field rainfall and runoff measurements in some catchments in the Kingdom of Saudi Arabia. Both stream flow data and synthetic techniques are used to derive the equations for the Ari-Zo model.

Study area

The study area is located within the Tehama escarpment of the Arabian Shield; it is characterized by semiannual flash floods (Bajabaa et al. 2014). Both of Allith and Yiba basins are located in the western part of the Kingdom of Saudi Arabia. Allith basin is located in the Makkah Al-Mukaramah region and it is about 200 km south of Jeddah city. It lies between 40° 10′ and 40° 50′ E and 20° 00′ and 21° 15′ N with an area of 3079 km^2, while Yiba basin is located in the Asir region. It is worth mentioning that the Yiba basin arises from Asir mountains of the Asir region and drains its water through the main channel towards the Makkah Al-Mukaramah region. It is about 380 km south of Jeddah city. It lies between 41° 15′ and 42° 10′ E and 18° 50′ and 19° 35′ N with an area of 2830 km^2 as shown in Fig. 1.

Geologically, Allith basin is underlain by late Proterozoic plutonic, meta-volcanic, and metasedimentary rocks in most of the basin with an area of about 86.8% of the total area, by chiefly Tertiary sedimentary, volcanic, and plutonic rocks in and near the coastal plain, and by Tertiary oceanic crust of the Red Sea offshore. The contact between continental and oceanic crust is probably 10–15 km onshore. Quaternary sediments of Aeolian sand, silt, and pediment deposits with an area of about 11.9% of the total area blanket the coastal plain with thickness that ranges from 2 to 10 m and were fringed by coral reefs that are uplifted locally along faults parallel to the coast (Pallister 1986; Cater and Johnson 1987).

The upstream of Allith basin is restricted between rugged mountainous terrains which get dissected by several tributaries which flow towards the main basin. The middle and the downstream of the basin are a low relief area covered by several types of Quaternary deposits including alluvium, sand plains, gravel, silt, and Aeolian sand dune fields, while the upstream has complicated relief covered by a relatively thin alluvium layer composed of sand and gravel (Pallister 1986; Cater and Johnson 1987).

Proterozoic age-layered and intrusive rocks, which are composed of gabbro, tonalite, granodiorite basalt and andesite, rhyolite, and green schist, surround the upper part of the basin. These hard rocks are characterized by a weathered surface covered with angular blocky fragments. Unconsolidated
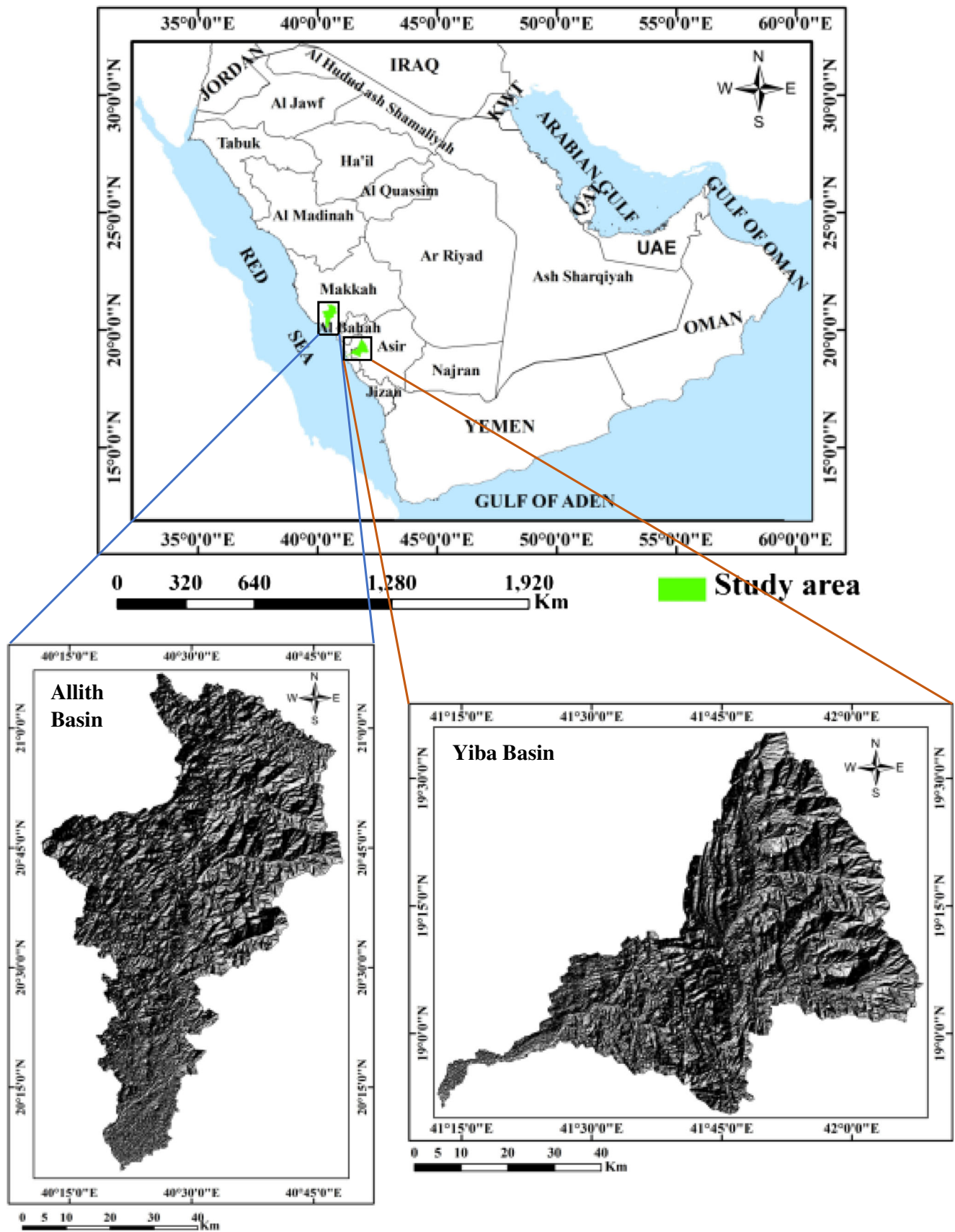
Fig. 1 Location of the study area and the relief maps of the basins in the current study

Quaternary deposits comprise the main alluvium deposits in the main channel and its tributaries (Pallister 1986; Cater and Johnson 1987).

Yiba basin is located in the Hali valley quadrangle area which is characterized by marine environment (Prinz 1984). Yiba basin is covered by late Proterozoic rocks (91.5%) and Quaternary rocks (8.5%). Late Proterozoic rocks comprise of metamorphic volcanic, sedimentary, and plutonic rocks while Quaternary rocks comprises Quaternary basaltic flows (lava) and wadi deposits (Prinz 1983, 1984; Greenwood et al. 1986).

The geomorphology of Allith basin shows a typical basin system flowing from the west part of the escarpment ridge of the Arabian Shield. It starts from the eastern high mountainous slopes of the escarpment and decreases down to the west of flat sediments of the Tehama coastal plain close to the Red Sea. The elevation of Allith basin ranges from 0 to 2620 m with a mean elevation of 824 m (above mean sea level, amsl). Allith basin

Table 1   Some morphometric parameters for Allith basin and its subcatchments

Parameter	Allith basin and its subcatchments				
	J-415	J-416	J-417	J-418	Allith basin
Area (A) (km²)	960.09	293.62	1692.75	2726.10	3079.00
Basin perimeter (B_P) (km)	221.73	92.88	302.60	432.68	586.57
Basin length (L_B) (km)	39.88	21.00	60.56	80.00	113.00
Valley length (L_V) (km)	45.64	17.23	73.75	15.72	60.78
Basin slope (S)	0.0548	0.0700	0.0404	0.0317	0.0232

and its surrounding areas exhibit different geomorphologic units as follows:

(a) The high mountainous area is composed essentially of Proterozoic rocks with high elevation values that reach to 2620 m (amsl), which is representing the main catchment of the basin. The high mountainous area of the study area plays an important role in the rainfall intensity.

(b) The hilly area occupies the northeastern and middle parts of the basin. This area is composed of a hilly dissected and weathered zone as shown in Fig. 1.

(c) The coastal plain occupies the low land area between the mountainous area and the Red Sea. It comprises morph tectonic depressions and the main channel of the basin.

Tihama Asir, where Yiba basin is located, is characterized by three distinct geomorphologic features which show different hydrological units as follows:

(a) Asir mountain range is elevated of about 2700 m above mean sea level and extends north to south parallel to the Red Sea. The mountains are cut by deep basins,
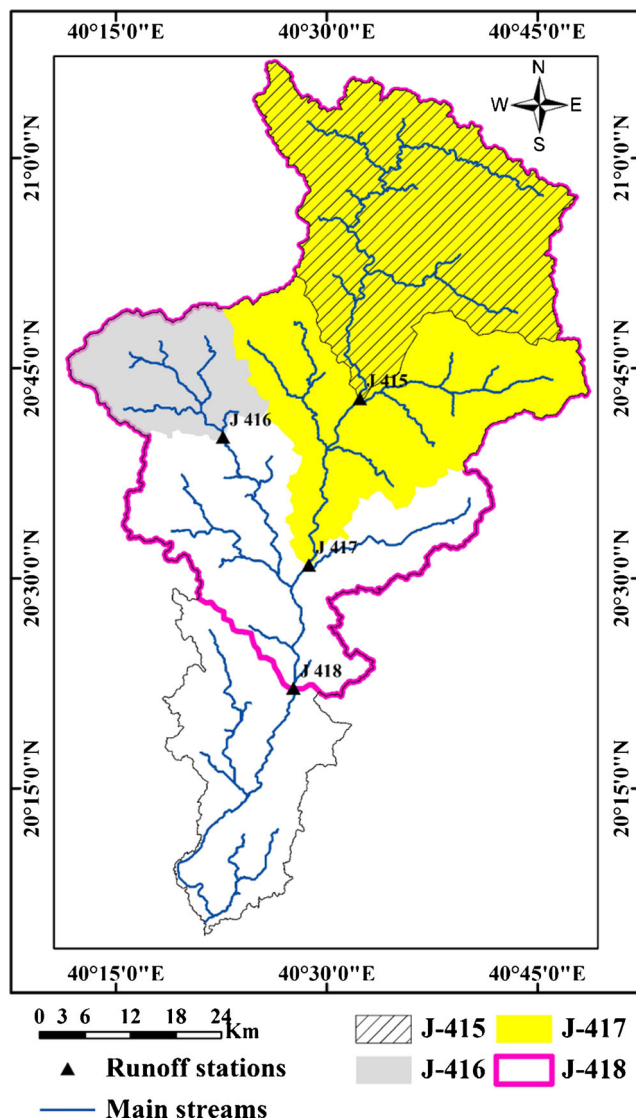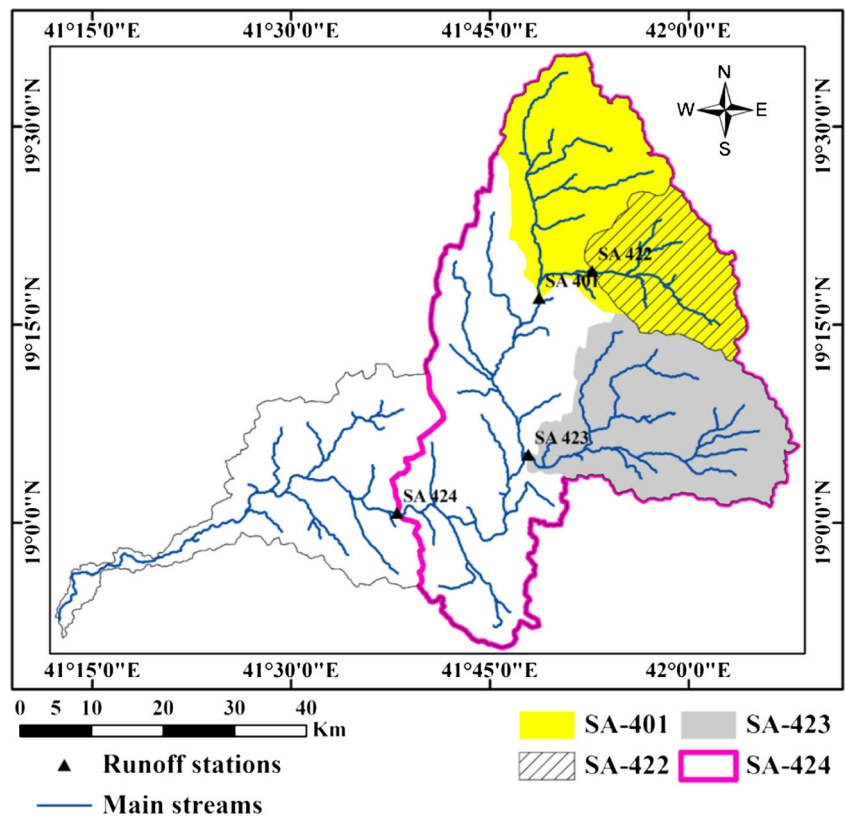

Fig. 2 Allith basin and its subbasins with the stream network

Table 2   Some morphometric parameters for Yiba basin and its subcatchments

Parameter	Yiba basin and its subcatchments				
	SA-422	SA-422	SA-422	SA-422	Yiba basin
Area (A) (km²)	307.00	762.92	611.84	2338.30	2830.00
Basin Perimeter (B_P) (km)	77.76	138.16	118.01	274.77	393.97
Basin length (L_B) (km)	18.70	26.00	34.00	56.00	99
Valley length (L_V) (km)	5.37	2.25	18.41	64.79	132.48
Basin slope (S)	0.1151	0.0876	0.0713	0.0458	0.0272

Fig. 3 Yiba basin and its subbasins with the stream network

meandering towards the coastal plain, which provides communications within the mountains.

(b) The foothill area bordering the eastern side is covered mostly by gravels and depressions filled with alluvial deposits and has good potentiality for water recharge. This area is gently sloping with some vegetation. Tributaries of Yiba basin, which originate in the Asir mountains, cross the foothills to the coastal plain as shown in Fig. 1.

(c) Coastal plain is restricted between the sabkhas along the Red Sea coast and the foothills, where the agricultural activity is taking place along the basins. This plain is characterized by alluvial deposits (Abu-Alainine 1979; Al-Sharif 1977). Coastal plain varies in width from 10 to 65 km and is bounded from the east by a massive rugged mountain of igneous and metamorphic rocks which is elevated about 400 m above mean sea level.

Fig. 4 A phi (Φ) index approach for determining the effective rainfall from a rainstorm (example: station SA-423 with a storm on 7 Jun 1986)
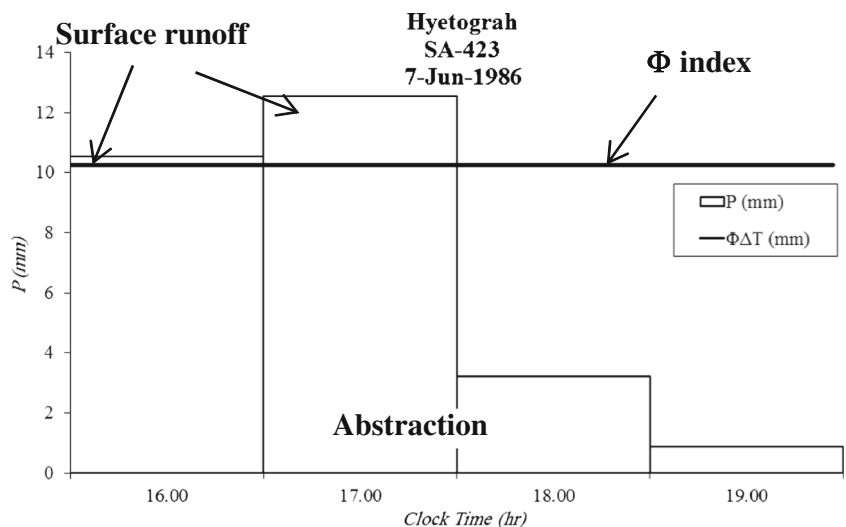
Fig. 5 The storm hydrograph of the event on 7 June 1986 in SA-423 subcatchment and its corresponding unit hydrograph
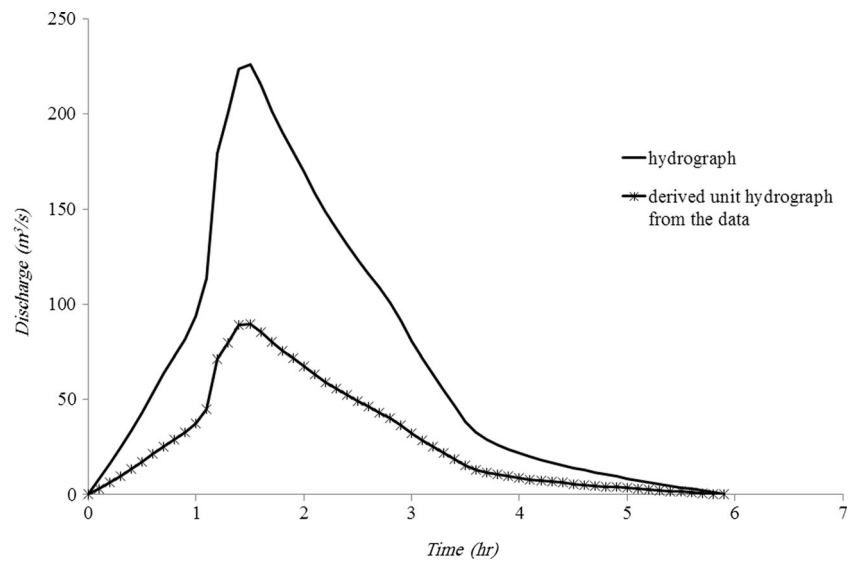

Figure 2 shows locations of Allith basin and its subcatchments. Some of their morphometric parameters are tabulated in Table 1. Figure 3 shows locations of Yiba basin and its subcatchments. Some of their morphometric parameters are tabulated in Table 2.

Methodology

The procedure to derive the unit hydrograph comprises the following steps:

1. Storm selection: a measured storm hydrograph has been selected from the recorded data. The selection is based on the hydrograph having a single peak, the flow caused by a connected excess rainstorm without gaps, and the rainstorm occurring after a dry period. A storm at station

SA-423 which has happened in 7 Jun 1986 has been selected as an example for illustration of the methodology.

2. Estimation of the direct runoff: a phi (Φ) index method is used to determine the effective rainfall (excess rainfall). The Φ index represents a constant (horizontal line) of intensity, which divides the rainfall intensity diagram in such a manner that the depth of rainfall above the index line is equivalent to the surface runoff depth over the basin. The portion of the rainfall intensity diagram below the line represents abstractions during the storm. Figure 4 shows the hyetograph of the storm and the Φ index line. The effective rainfall is 2.51 mm. The Φ index is obtained by subtracting the runoff volume obtained from a direct runoff hydrograph from the total rainfall during a storm such that (Raghunath 2006):

$$drv = \sum [max(0, I-\varnothing)]\Delta tA \tag{1}$$

Fig. 6 Oscillating phenomenon of the S-curve from the data and the fitted S-curve using the mathematical model proposed by Eq. 2
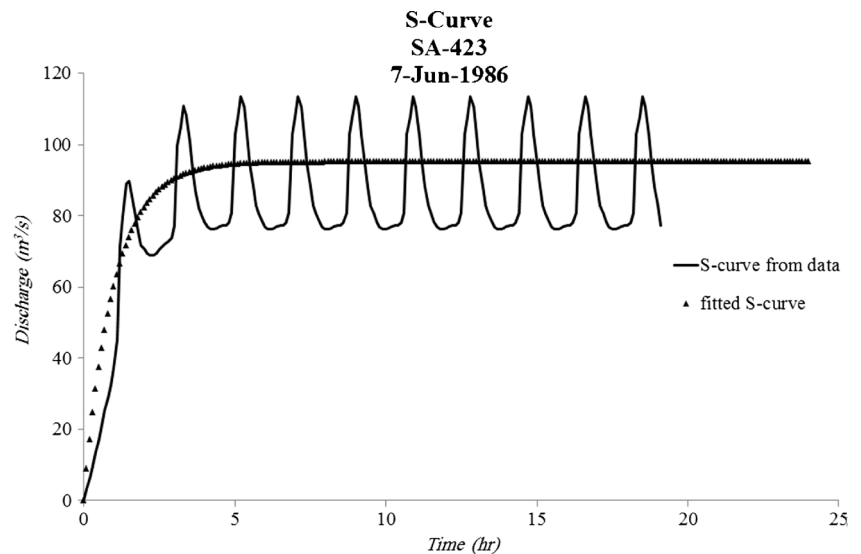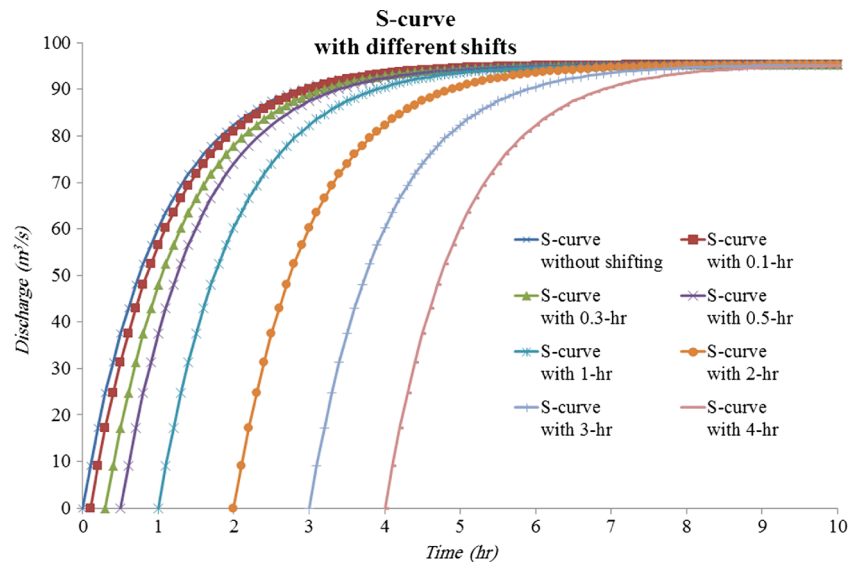
Fig. 7 The S-curve without shifting and the S-curve with different shifts (0.1, 0.3, 0.5, 1, 2, 3, and 4 h)

where

drv 　is the direct runoff volume (volume under direct runoff hydrograph);

I 　is the rainfall intensity during a period Δt;

Δt 　is the time interval of the rainfall intensity in the data;

Φ 　is the phi index; and

A 　is the drainage basin area.

3. Calculation of the unit hydrograph: the unit hydrograph is calculated by dividing each value in the hydrograph ordinate on the value of effective rainfall depth. Figure 5 shows the storm hydrograph of the event on 7 June 1986 and its corresponding unit hydrograph. It is noted that this unit hydrograph is a 2-h duration.

4. Estimation of the S-curve: S-curve is the hydrograph of direct runoff that would result from a continuous succession of unit storms producing 1-unit depth in the duration of the unit hydrograph. It was created for each storm to derive unit hydrograph of different durations from all storms. It is noticed that high oscillations appeared in the S-curve as shown in Fig. 6. This is a known phenomenon in S-curve (Hunt 1985). Hunt has proved the existence of these oscillations, in certain cases. To overcome this problem, a representation of the S-curve by a differential equation in a time-independent manner is proposed by Hunt (1985). For more details regarding this issue, the reader may refer to Hunt (1985). Therefore, it is necessary to synthesize a mathematical model to represent such an S-curve. It is assumed as an

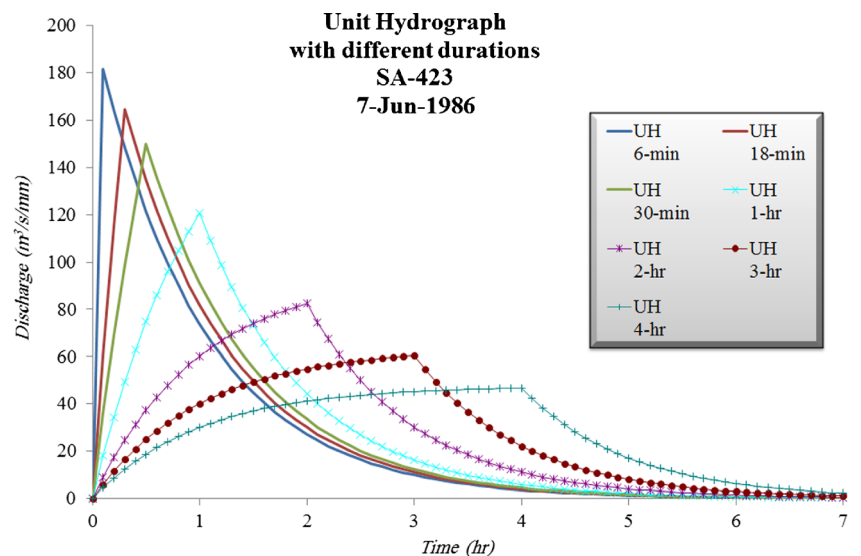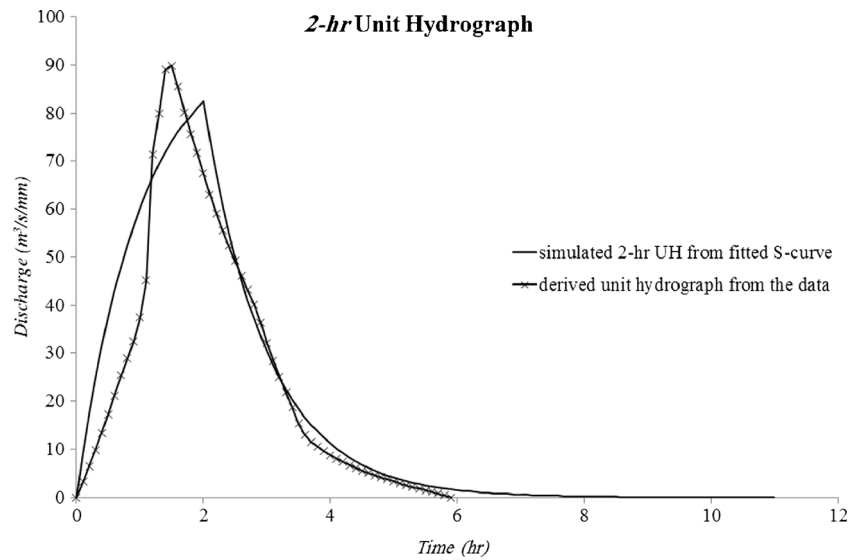**Fig. 8** The unit hydrograph of different durations

Fig. 9 The simulated (from S-curve) and the derived (from data) 2-h unit hydrograph

exponential equation in the form of Eq. 2 for that purpose,

$$Q = a\left(1-e^{-bt}\right) \tag{2}$$

where

Q is the discharge (m³/s);
a is a fitting parameter estimated from the variance of the data;
e is the base of the natural logarithms;
b is another fitting parameter related to the steepness of the curve at the origin; and
t is the time (h).

Figure 6 shows the fitting of the aforementioned equation to the actual S-curve. After using this mathematical model, a hydrograph of certain duration can be obtained.

5. Calculation of a unit hydrograph of any specified duration: in order to derive a unit hydrograph of specific duration, the S-curve has to be shifted with the required duration. Figure 7 shows the shift of the S-curve with durations 0.1, 0.3, 0.5, 1, 2, 3, and 4 h and the original S-curve without shifting.

6. Estimation of the unit hydrograph of various durations: the unit hydrograph of any duration is made by applying the following equation (Raghunath 2006),

$$Q = \frac{D(S_{C_0} - S_{C_1})}{t} \tag{3}$$

where

Q is the discharge;
D is the original duration of the unit hydrograph;
S_{C_0} is the S-curve without shifting;

Fig. 10 Derivation of the unit hydrograph of 1-h duration from S-curve

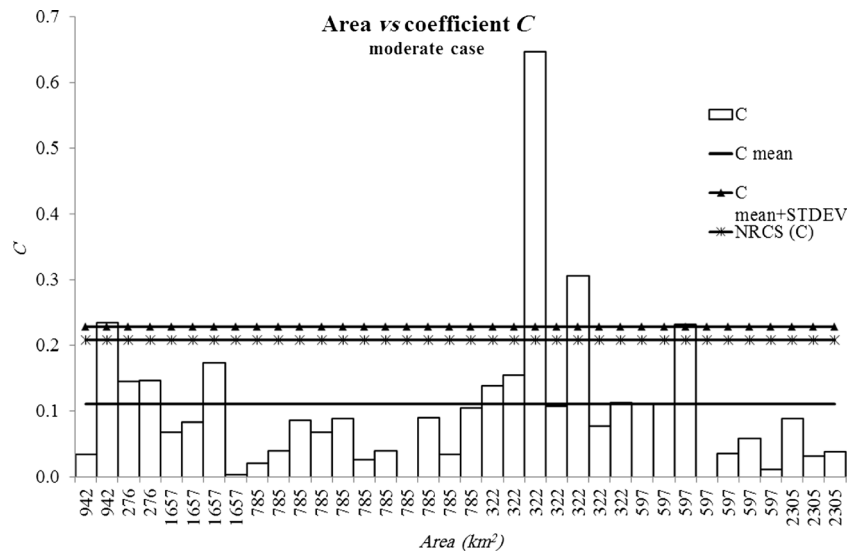**Fig. 11** The average peaking factor (C) in very extreme case and its upper limit confidence interval compared with the commonly used peaking factor of the NRCS method

S_{C_1} is the S-curve after shifting; and
t is the desirable duration.

Figure 8 represents the unit hydrographs of different durations.

Figure 9 shows a comparison between the unit hydrograph of 2-h storm duration that is derived using the fitted S-curve given in Fig. 6 and Eq. (3) and the one that is obtained from the data. It is noticed in the figure that the unit hydrographs are slightly different from each other due to the smoothing effect in S-curve made by the fitting. Figure 10 shows the simulated 1-h unit hydrograph resulting from shifting the S-curve for 1 h.

After constructing the unit hydrographs from all storms and at all stations and subcatchments, empirical equations are developed. Mathematical relationships are derived between the

hydrological variables of the unit hydrograph and the morphological parameters, with the involvement of the time factor.

Relationships have been established between time to peak and time of concentration, time of concentration and slope of the basins, and peaking factors for peak flow estimation. The established relationships are compared with those in the NRCS method. The following sections provide detailed discussions of these formulas.

Results and discussions

Peaking factors for Ari-Zo model (C)

The famous equation of NRCS in 1972 (NRCS 1972 referenced by Viessman et al. 1977 and Viessman and Lewis

Fig. 12 The average peaking factor (C) in the extreme case and its upper limit confidence interval compared with the commonly used peaking factor of the NRCS method

Fig. 13 The average peaking factor (C) in the moderate case and its upper limit confidence interval compared with the commonly used peaking factor of the NRCS method

2002) to calculate the peak discharge of the unit hydrograph (Q_P) using the drainage basin area (A) and the time to peak (T_P) is as follows:

$$Q_P = \frac{C \cdot A}{T_P} \tag{4}$$

where

Q_P is the peak discharge of the unit hydrograph (m³/s/mm);
C is the peaking factor;
A is the basin area (km²); and
T_P is the time to peak (h).

There are several peaking factor values in the NRCS method. Nevertheless, there is a famous value that is commonly used in practice which is equal to 484 in imperial units or 0.2083 in metrics units. The current

study produced four values of the peaking factor for different flow regimes. The peaking factor is estimated by rearranging Eq. 4 as,

$$C = \frac{Q_P \cdot T_P}{A} \tag{5}$$

Given the items in the right-hand side of the equation, the peaking factor is estimated for each rainfall event and plotted for the area of the drainage basin. The following sections discuss the peaking factors in details.

Very extreme case (C_{VE})

In this case, the highly severe events have been used to estimate the very extreme peaking factor, while the remaining values have been ignored. Figure 11 shows a

Fig. 14 The average peaking factor (C) in low case and its upper limit confidence interval compared with the commonly used peaking factor of the NRCS method
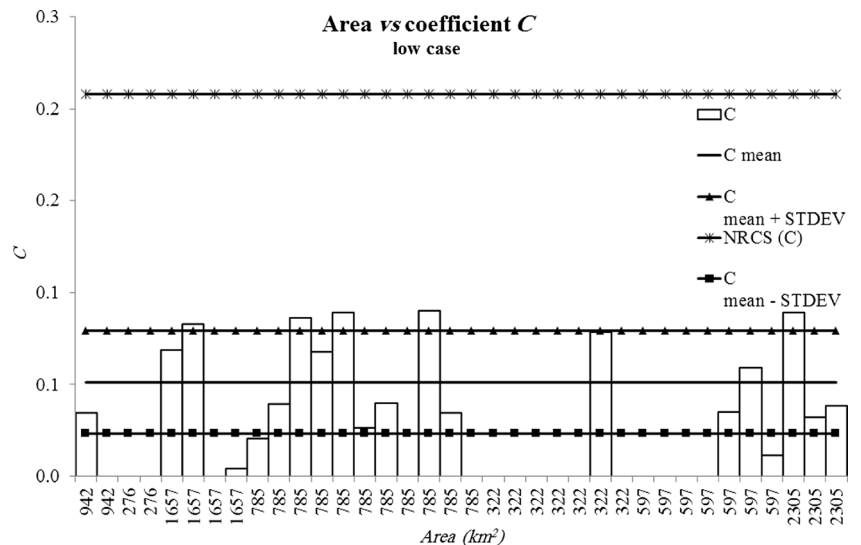
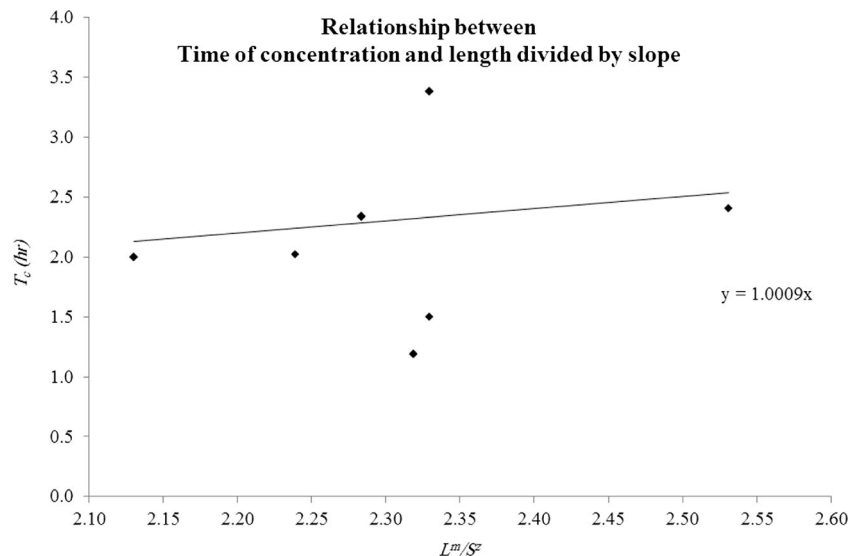**Table 3** Comparison between NRCS method and Ari-Zo model peaking factors

NRCS peaking factors (metric units)	Ari-Zo peaking factors (metric units)	Remarks
	0.0513	Low case
0.0646		
	0.1103	Moderate case
0.1291		
0.1592		
0.1721		
0.1937		
0.2083		Commonly used
0.2152		
0.2367		
0.2582		
	0.2994	Extreme case
	1.9465	Very extreme case

plot between the drainage basin area and the peaking factor for every event. The average of the peaking factor in the very extreme case is equal to 1.9465. It is advised to use this value in the case of very extreme floods (Q ≥ 500 m^3/s/mm).

Extreme case (C$_E$)

The second value is resulted in an extreme flood regime. In this case, all the data have been used without omitting any extreme values as shown in Fig. 12. The average peaking factor is equal to 0.2994 in the extreme case. It is advised to use this value in the case of high floods (500 m^3/s/mm > Q ≥ 150 m^3/s/mm).

Moderate case (C$_M$)

The third value is resulted in a moderate flood regime. In this case, the extreme values have been omitted in order to improve the results as indicated in Fig. 13. The average peaking factor is equal to 0.1103 in the moderate case. This value is used in the case of medium flood regime (90 m^3/s/mm ≤ Q < 150 m^3/s/mm).

Low case (C$_L$)

The fourth peaking factor resulted in a low flood regime. In this case, the values of the peaking factor greater than 0.1 are omitted to get a smaller peaking factor proportional to the small floods as shown in Fig. 14. The average of the peaking factor is equal to 0.0513 in the low case. It is advisable to use this value when the peak discharge is less than 90 m^3/s/mm.
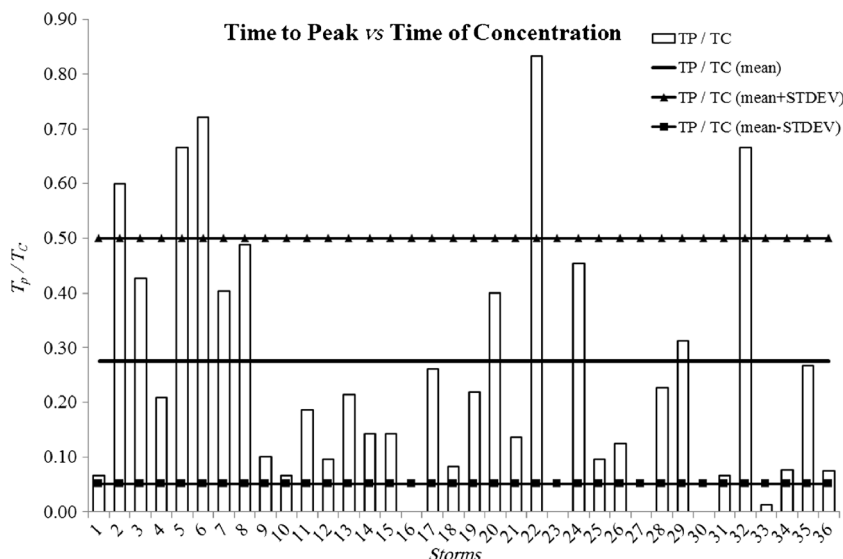
From the above analysis, it is clear that the peaking factor in arid regions varies significantly between the very extreme case and the low case. It is also noticeable that it is completely different from the NRCS method.

The coefficient C in the Eq. 4 has four values to be used in arid zones. These values are summarized as follows:

– 1.9465 (very extreme case)
– 0.2994 (extreme case)
– 0.1103 (moderate case)
– 0.0513 (low case)

The NRCS method has nine values of the peaking factor (NRCS 1972 referenced by Fang et al. 2005). Table 3 summarizes a comparison between the Ari-Zo peaking factors with the aforementioned cases and the corresponding NRCS peaking factors.

Fig. 15 Relationship between the time of concentration (T$_C$) averaged over the storms for each subcatchment and the length of the main stream (L), divided by the basin slope (S)

Fig. 16 The relationship between T_P and T_C

Topography effect on the time of concentration (T_C)

The time of concentration is the time for a drop of water to flow from the hydraulically most remote point in the watershed to the outlet. It is clear from the definition of the relationship between the basin slope and time of concentration. This relationship is inversely proportional to the basin slope. Proceeding from this concept, the scientists derived many empirical equations to calculate the time of concentration using the topographic information for each basin. It is necessary to derive an empirical equation to calculate this time in arid zone basins. The time of concentration for each storm can be estimated from the storm center to the inflection point of the hydrograph.

Figure 15 shows a plot between the time of concentration averaged over the storms for each subcatchment and the basin length to the power m and the basin slope to the power z.

The empirical equation resulting from the plot is in the form,

$$T_C = \frac{L^m}{S^z} \tag{6}$$

where

T_C	is the time of concentration (h);
L	is the basin length (km); and
S	is the basin slope (m/m).
m	equals to 0.09
z	equals to 0.11

Relationship between the time to peak (T_P) and the time of concentration (T_C)

The ratio between the time to peak and time of concentration for each storm has been evaluated and plotted against each storm. Then, the average has been calculated. Figure 16 shows the relationship between the ratio of the time to peak and the time of concentration. The solid line represents the average value of this ratio which is equal to 0.276. The upper line with the triangular symbols is the average plus the standard deviation of the ratio. The lower line with square symbols is the average minus the standard deviation of the ratio.

The equation for the average ratio is as follows:

$$T_P = 0.276\ T_C \tag{7}$$

Table 4 Summary for the comparison between of the NRCS equations and the Ari-Zo equations

	NRCS	Ari-Zo
Peak discharge (Q_P)	$Q_P = \frac{C \cdot A}{T_P}$	$Q_P = \frac{C \cdot A}{T_P}$
	$C = 0.0646 \quad C = 0.1291$	$C = 0.0513$ (low)
	$C = 0.1592 \quad C = 0.1721$	$C = 0.1103$ (moderate)
	$C = 0.1937 \quad C = 0.2083$	$C = 0.2994$ (extreme)
	$C = 0.2152 \quad C = 0.2367$	$C = 1.9465$
	$C = 0.2582$	(very extreme)
Time of concentration (T_C)	$T_C = \frac{T_L}{0.6}$	$T_C = \frac{L^{0.09}}{S^{0.11}}$
		(metric system)
	$T_L = \frac{L^{0.8}(M+1)^{0.7}}{1900\sqrt{S}}$	
	$M = \frac{25400}{CN} - 254$	
	(metric system)	
	$T_C = 0.0663\left(\frac{L}{\sqrt{S}}\right)^{0.77}$	
	(Kirpich 1940)	
	[T_C (h) & L (km)]	
Time to peak (T_P)	$T_P = \frac{2}{3}T_C$	$T_P = 0.276 T_C$
		min. $T_P/T_C = 0.05$
		max. $T_P/T_C = 0.5$

where

T_P is the time to peak (h) and
T_C is the time of concentration (h).

Due to the high variation observed in Fig. 16, the ratio between the time to peak and time of concentration varies between 0.05 and 0.5.

Table 4 summarizes the comparison between the NRCS equations and the Ari-Zo equations. From this comparison, a dramatic difference is found between the parameters in both methods for the peaking factor, the time of concentration equation, and the time to peak.

Conclusions

Empirical equations for flood analysis in arid zones have been established. These equations are called the Ari-Zo model. The equations are derived based on rainfall and runoff measurements (36 storms) at some stations at catchment outlets (eight subbasins) in the southwestern part of Saudi Arabia. The parameters estimated from this study are dramatically different from the ones that have been estimated in temperate conditions. The peaking factors of NRCS range between 0.0646 and 0.2582, while in Ari-Zo, it ranges between 0.0513 (low flood case) and 1.9465 (very extreme flood case). The ratio between the time to peak and the time of concentration in NRCS is equal to 0.667, while in Ari-Zo, it ranges between 0.05 and 0.5 and on average, it is 0.276. The parameters of time of concentration in the Ari-Zo model are different from those of Kirpich equation. The study recommends using the Ari-Zo model for arid zone hydrological studies. Application of the model for simulation of some events will be considered in future studies.

References

Abu-Alainine HA (1979) Geomorphology, Beirut, Dar Al-Nahdah Al-Arabia, 5th Edition. In Arabic

Albishi M (2015) Unit hydrograph of watersheds in arid zones: case study in south western Saudi Arabia, MSc Thesis, King Abdulaziz University, Saudi Arabia

Alriyadh Newspaper (2011) vol. 15559 in 29/01/2011. Available at http://www.alriyadh.com/599456. Accessed May 17, 2015

Al-Sharif AS (1977) Geography of Saudi Arabia, Riyadh, Dar Al-Marrekh Press, vol.1, In Arabic

Al-watan online news (2010) in 10/05/2010. Available at http://www.alwatan.com.sa/Local/News_Detail.aspx?ArticleID=1623&CategoryID=5. Accessed Nov 8, 2015

Bajaaa S, Masoud MH, Al-Amri N (2014) Flash flood hazard mapping based on quantitative hydrology, geomorphology and GIS techniques (case study of Wadi Al Lith, Saudi Arabia). Arab J Geosci 7:2469–2481

Bhunya PK, Mishra SK, Berndtsson R (2003) Simplified two-parameter gamma distribution for derivation of synthetic unit hydrograph. Journal of Hydrology Engineering 8:226–230

Cater FW, Johnson PR (1987) Geologic map of the Jabal Ibrahim quadrangle, Sheet 20E, Kingdom of Saudi Arabia: Saudi Arabian Deputy Ministry for Mineral Resources Geologic Map GM 96, scale 1:250,000

Clark CO (1945) Storage and the unit hydrograph. Transactions of American Society of Civil Engineers 110:1419–1446

Edson CG (1951) Parameters for relating unit hydrograph to watershed characteristics. Trans Am Geophys Union 32(4):591–596

Fang X, Prakash K, Cleveland T, Thompson D, Pradhan P (2005) Revisit of NRCS Unit Hydrograph Procedures, (Proceedings of the ASCE Texas Section Spring Meeting) Austin, Texas. Available at: http://cleveland2.ce.ttu.edu/documents/copyright/ and http://www.eng.auburn.edu/~xzf0001/Publications.htm. Accessed April 21, 2015

Gray DM (1961) Synthetic Unit Hydrographs for Small Drainage Areas, Proceeding American Society of Civil Engineers, vol. 87

Greenwood WR, Jackson RO, Johnson PR (1986) Geologic map of the Jabal Al-Hasir quadrangle, Sheet 19F, Kingdom of Saudi Arabia: Saudi Arabian Deputy Ministry for Mineral Resources Geologic Map GM 94, scale 1:250,000

Hunt B (1985) The meaning of oscillations in unit hydrograph S-curves. Hydrol Sci J 30:331–342

Kirpich ZP (1940) Time of concentration of small agricultural watersheds, Civil Engineering Journal. vol. 10, No. 6

McCuen RH, Johnson PA, Ragan RM (2002) Highway hydrology, 2nd edn. U.S. Department of Transportation, Washington, D.C.

Mockus V (1957) Use of storm and watershed characteristics in synthetic hydrograph analysis and application, Washington D.C.: U.S. Department of Agriculture, Soil Conservation Services

Natural Resources Conservation Services (1972) National Engineering Handbook, Section 4: Hydrology, Washington D.C.: U.S. Department of Agriculture

Okaz Newspaper (2014) vol. 4709 in 09/05/2014. Available at: http://www.okaz.com.sa/new/Issues/20140509/Con20140509698234.htm. Accessed May 4, 2015

Pallister JS (1986) Geologic map of the Al-Lith quadrangle, Sheet 20D, Kingdom of Saudi Arabia: Saudi Arabian Deputy Ministry for Mineral Resources Geoscience Map GM 95C, scale 1:250,000

Prinz WC (1983) Geologic map of the Al Qunfudhah quadrangle, Sheet 19E, Kingdom of Saudi Arabia: Saudi Arabian Deputy Ministry for Mineral Resources Geologic Map GM 70, scale 1:250,000

Prinz WC (1984) Geologic map of the Wadi Haliy quadrangle, Sheet 18E, Kingdom of Saudi Arabia: Saudi Arabian Deputy Ministry for Mineral Resources Geologic Map GM 74, scale 1:250,000

Raghunath HM (2006) Hydrology. New Age International, New Delhi

Sherman LK (1932) Stream-flow from rainfall by the unit-graph method. Engineering News-Record 105:501–505

Singh PK, Jain MK, Mishra SK (2011) Fitting a simplified two-parameter gamma distribution function for synthetic sediment graph derivation from ungauged catchments. Arab Journal of Geosciences 6:1835–1841

Snyder FF (1938) Synthetic unit graphs. Transactions American Geophysical Union 19:447–454

Viessman JW, Lewis GR (2002) Introduction to hydrology, 5th edn. Prentice Hall, Bergen

Viessman JW, Knapp JW, Lewis GR, Harbaugh TE (1977) Introduction to hydrology, 2nd edn. Harper & Row, New York